April 2004

Structural and magnetic properties of Y0.33Sr0.67CoO2.79

D. J. Goossens
Australian National University

K. F. Wilson
University of New South Wales

M. James
ANSTO, Australia

A. J. Studer
ANSTO, Australia

Xiaolin Wang
University of Wollongong, xiaolin@uow.edu.au

Structural and magnetic properties of $Y_{0.33}Sr_{0.67}CoO_{2.79}$

D. J. Goossens*
Research School of Chemistry, Australian National University, Canberra, Australian Capital Territory 0200, Australia

K. F. Wilson
School of Physics, University of New South Wales, Sydney 2052, Australia

M. James and A. J. Studer
The Bragg Institute, Australian Nuclear Science and Technology Organization, Lucas Heights, New South Wales 2234, Australia

X. L. Wang
Institute for Superconducting and Electronic Materials, University of Wollongong, Wollongong, New South Wales 2522, Australia
(Received 20 October 2003; revised manuscript received 20 January 2004; published 6 April 2004)

The perovskite-based oxide $Y_{0.33}Sr_{0.67}CoO_{2.79}$ has been magnetically and structurally characterized. The material shows a unit cell of $2\times2\times4$ simple perovskite cubes with space group $I4/mmm$. This is a different structure to that observed in the much-studied $(La,Sr)CoO_3$ oxides. Oxygen stoichiometry is established through thermogravimetric analysis and correlated with ac and dc magnetic measurements and magnetic neutron diffraction. Hysteresis with field and temperature is observed in the dc magnetization measurements, yet the absence of an imaginary component in the ac susceptibility suggests a time-independent cause for these effects such as the presence of independently ordering ferromagnetic regions due to compositional inhomogeneities within the (single-phase) sample. Rietveld magnetic refinements suggest that the Co moments are arranged antiferromagnetically below 320 K, with the ferromagnetic regions existing within the long-range ordered antiferromagnetic matrix. The staggered moments are (anti)parallel with the *c* axis and of magnitude $2\mu_B$, a moment most typical of intermediate spin Co^{3+}. The material does not enter a spin glass or cluster glass phase, but appears to undergo a broad spin-state transition below 100 K.

DOI: 10.1103/PhysRevB.69.134411 PACS number(s): 75.50.Gg, 75.50.Lk, 75.30.Cr, 61.12.Ld

I. INTRODUCTION

Perovskite-based oxides are an important class of materials, much studied in recent times, and include the high-T_c superconductors and the colossal magnetoresistance manganites. Also of technological relevance and scientific interest are the rare-earth strontium cobaltates, $Ln_{1-x}Sr_xCoO_{3-\delta}$ (Ln = lanthanide ion). These materials are being studied for possible applications in solid oxide fuel cells[1–4] and as membranes for gas separation.[5,6] The materials show a range of magnetic behavior including glassiness[7] and ferromagnetism.[8] $La_{1-x}Sr_xCoO_{3-\delta}$ has been extensively studied (Refs. 7 and 9–14, for example). Recently interest has increased in perovskite-related phases with smaller lanthanide ions,[15] but few systematic studies of these phases exist. The work presented here is part of a systematic study of the structure and magnetic properties of this large family of compounds.[16,17] The physical properties of these materials are strongly dependent upon composition as well as ionic and oxygen vacancy ordering. Oxygen ionic conductivity, for example, is known to be affected by oxygen vacancy ordering and associated structural relaxation;[3] magnetic behavior will be affected by the Co^{3+}/Co^{4+} ratio and distribution. Samples for which $Ln^{3+}=Y^{3+}$ are ideal for this study as Y is non-magnetic, like the La used in other studies, but is quite different in ionic size [Ref. 18 tabulates $r_{ion}(Sr^{2+})=1.31$ Å, $r_{ion}(Y^{3+})=1.075$ Å, and $r_{ion}(La^{3+})=1.216$ Å, for coordination number = 9; unfortunately, there is no listing for 12-fold coordinated Y^{3+}]. It has been shown that the crystal structure of $Ln_{0.33}Sr_{0.67}CoO_{3-\delta}$ is consistent across Ln = Dy, Ho, and Y,[16] so the determination of the magnetic structure of $Y_{0.33}Sr_{0.67}CoO_{2.79}$ has the benefit of some generality, while Y^{3+} is also convenient for neutron-diffraction studies. Although lacking x-ray contrast compared with Sr^{2+}, its neutron-scattering length is 10% different [$b_{coh}(Y^{3+})=7.75$ fm, $b_{coh}(Sr^{2+})=7.02$ fm, Ref. 19], which is not large but is an improvement over the x-ray case. Compared with other lanthanides of similar size, Y lacks the paramagnetic $4f$ electrons and has a small absorption cross section [$\sigma_{abs}(Y^{3+})=1.28$ b, $\sigma_{abs}(Ho^{3+})=64.7$ b, $\sigma_{abs}(Dy^{3+})=994$ b, and $\sigma_{abs}(Gd^{3+})\sim49\,700$ b].

II. EXPERIMENT

A. Synthesis

A polycrystalline sample of $Y_{0.33}Sr_{0.67}CoO_{3-\delta}$ was prepared from powders of $SrCO_3$ (98+%), $Co(NO_3)_2.6H_2O$ (98%), and Y_2O_3 (99.9%). The powders were dissolved in dilute nitric acid and a mixture of the metal oxides was formed via the decomposition of a citric acid-ethylene glycol sol gel. The residues were pelleted and sintered at 1100 °C under flowing oxygen for up to three days with intermediate regrinding and repelleting until no further reaction was evident by x-ray powder diffraction.

B. Thermogravimetry

Thermogravimetry of ca. 70 mg samples of $Y_{0.33}Sr_{0.67}CoO_{3-\delta}$ was carried out at ANSTO using a

SETARAM TAG24 simultaneous thermogravimetric analysis(TGA) and differential thermal analysis(DTA). Samples were reduced under 3.5% hydrogen in nitrogen over a temperature range of 25–900 °C at a heating rate of 5 °C/min. After complete reduction of the sample, Y and Sr are present as Y_2O_3 and SrO, respectively. Measurement of the mass of oxygen lost as the cobalt is reduced to Co(0) metal enables calculation of the oxygen defect, δ, for the as-prepared sample.[20]

C. X-ray powder diffraction

Synchrotron x-ray powder diffraction (XRD) patterns were collected at the Australian National Beamline Facility, Tsukuba, Japan. Samples were mounted in 0.5 mm quartz capillaries and data were collected in transmission geometry with $\lambda = 0.998\,68$ Å using an image plate detector. Structural refinements used the Rietveld approach[21] implemented in Rietica[22] with pseudo-Voigt peak shapes and a refined background.

D. Magnetic measurements

ac magnetic susceptibility was measured using a Lakeshore 7000 series ac susceptometer (School of Physics, University of New South Wales, Australia) with a closed cycle helium refrigerator (CCR) ($17\ \mathrm{K} < T < 323\ \mathrm{K}$). Measurements were made in drift mode with a heater switched on manually when the sample reached room temperature. Maximum rms magnetic field was 20 Oe and ac frequency could be varied from 1 Hz to 10 kHz. Blank runs were performed to allow for the response of the sample holder.

dc magnetization was measured using a Quantum Design MPMS-7 superconducting quantum interference device magnetometer (Institute for Superconducting and Electronic Materials, University of Wollongong, Australia) with a 7 T superconducting magnet, capable to temperatures from 4.2 K to 350 K.

In both cases the samples consisted of small volumes of powder, ca. 30 mg, contained in nonmagnetic Teflon sample holders.

E. Neutron powder diffraction

Neutron powder-diffraction (ND) data were collected at 1.6677 Å using the MRPD diffractometer at the HIFAR research reactor, Lucas Heights, Australia. Approximately 4 g of powder was loaded into an 8 mm vanadium sample can which was mounted in a CCR capable of temperatures varying from 10 to 480 K. ND data were collected at 10, 50, 55, 60, 100, 200, 290, 300, 350, 400, and 480 K. These data were analyzed using the FULLPROF program[23] which allows Rietveld refinement of magnetic structures.

III. RESULTS AND DISCUSSION

A. XRD and TGA

TGA results showed that $\delta = 0.21 \pm 0.01$ which suggests that 25% of the Co ions are Co^{4+}. This small fraction implies that the dominant magnetic interaction in the system should be the antiferromagnetic Co^{3+}-Co^{3+} double exchange.

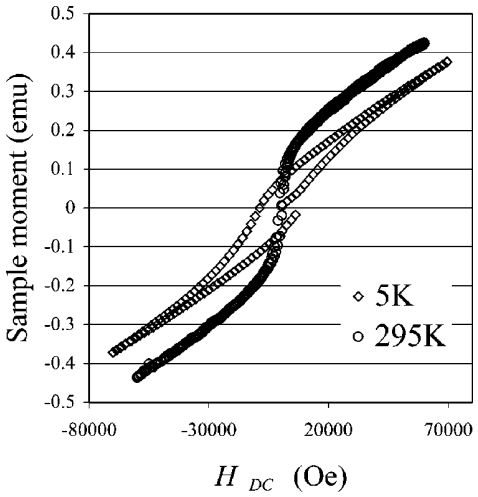

FIG. 1. *M-H* loops for a polycrystalline sample of $Y_{0.33}Sr_{0.67}CoO_{2.79}$ at 5 and 295 K.

Synchrotron XRD was used to determine the structure of $Y_{0.33}Sr_{0.67}CoO_{2.79}$, and a detailed structural description has been published.[16] The spacegroup is tetragonal $I4/mmm$ with lattice parameters $a = 7.6282(2)$ and $c = 15.3337(4)$ Å at 295 K. Other recent work on $Sr_{0.7}Y_{0.3}CoO_{2.62}$ independently gives the same unit cell ($2 \times 2 \times 4$ perovskite cubes) as Ref. 16 and the same space group.[24] The $Sr_{0.7}Y_{0.3}CoO_{2.62}$ samples used in Ref. 24 were prepared using conventional solid-state synthesis rather than sol gel and were fired under air rather than 1 atm of O_2, resulting in different oxygen stoichiometry. This may explain why the conclusions in Ref. 24 differ from those in Ref. 16 and in this work (Sec. III C) regarding the distribution of oxygen vacancies. It would also be expected to lead to very different magnetic properties, as the average cobalt oxidation state is very different.

The lack of contrast between Y^{3+} and Sr^{2+} means that the superstructure peaks in the XRD profile are primarily due to oxygen vacancy ordering. In the x-ray experiments, Ln^{3+}/Sr^{2+} ordering was established through studies of isostructural $Ho_{0.33}Sr_{0.67}CoO_{3-\delta}$ and $Dy_{0.33}Sr_{0.67}CoO_{3-\delta}$ phases. These results agree with the Y^{3+}/Sr^{2+} ordering observed in the neutron-diffraction study (Sec. III C, below).

B. Bulk magnetic measurements

Figure 1 shows magnetization versus applied field loops for a polycrystalline sample of $Y_{0.33}Sr_{0.67}CoO_{2.79}$. The loop at 295 K is very narrow, indicating that the ordering temperature is close to 295 K. The moment does not saturate for $H = 70$ kOe at any of the measured temperatures. The figure shows the two extreme cases—5 K and 295 K—and for both there is an increase in M with H at fields for which the hysteresis loops are closed.

Section III C shows that the magnetic structure is correlated antiferromagnetically, while the existence of the hysteresis loop implies a ferromagnetic component, suggesting an

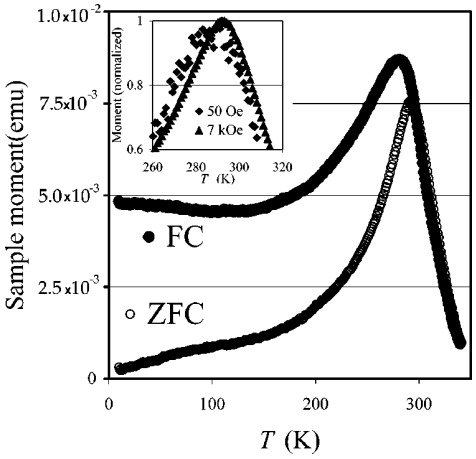

FIG. 2. Zero-field cooled (ZFC) and field cooled (FC) magnetizations against T for a polycrystalline sample $Y_{0.33}Sr_{0.67}CoO_{2.79}$ in a field of 7 kOe. Inset shows ZFC measurements in fields of 50 Oe and 7 kOe normalized to demonstrate the constant cusp width.

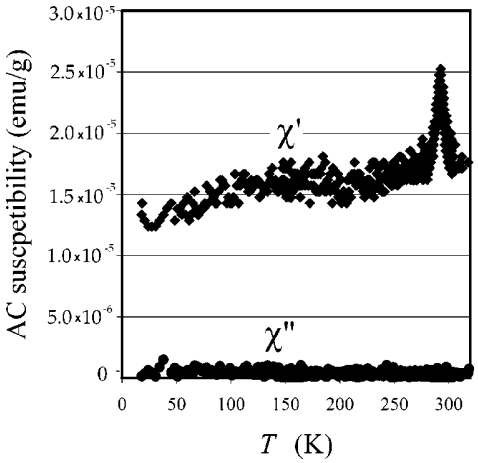

FIG. 3. ac susceptibility of a polycrystalline sample of $Y_{0.33}Sr_{0.67}CoO_{2.79}$ with $H_{AC}=6.25$ Oe, $H_{DC}=0$, and $f=125$ Hz.

overall ferrimagnetic material. The lack of saturation is sometimes related to glassiness,[11,25] although glasslike behavior in perovskite cobaltates has been ascribed to magnetocrystalline anisotropy as well.[14,26] In this case it will relate to the antiferromagnetism.

This behavior agrees with the model discussed in recent work on $La_{1-x}Sr_xCoO_3$,[12,27] which posits ferromagnetic clusters in a nonantiferromagnetic or antiferromagnetic matrix. Double exchange between Co ions of like oxidation state will produce an antiferromagnetic correlation, while Co^{3+}-Co^{4+} exchanges will be ferromagnetic. The TGA results, showing that 1/4 of Co sites are occupied by 4+ ions, suggest that ferromagnetic clusters within an antiferromagnetic matrix is the most likely model here.

The coercive field is $\approx$800 Oe at 295 K and 8.4 kOe at 5 K.

Figure 2 shows zero-field cooled (ZFC) and field cooled (FC) magnetizations for a polycrystalline sample of $Y_{0.33}Sr_{0.67}CoO_{2.79}$ versus temperature in an applied magnetic field of 7 kOe. Both curves show strong cusps ($T_c=295$ K for ZFC and 280 K for FC) indicative of a magnetic phase transition. From Fig. 1 this can be associated with ferromagnetism being present at temperatures below $\approx$295 K.

Figure 2 also demonstrates considerable thermomagnetic hysteresis, with the FC magnetization larger than the ZFC at all temperatures below the irreversibility temperature $T_{irr}=300$ K. This hysteresis has been observed previously in magnetic cobaltates (for example, Refs. 7, 13 and 27–29), and has been attributed to glassiness[28,7] and magnetocrystalline anisotropy.[14,29] In the anisotropy-based description, the ratio of the coercive field H_c at temperatures close to T_c to the applied field H_A is crucial in determining the shape of the magnetization curves. The divergence of FC from ZFC is ascribed to the opening up of hysteresis loops and a corresponding nonzero value for the coercivity as T falls. Further, it is suggested that a magnetization measurement made such that $H_A \sim H_c$ would show a very broad peak in the ZFC magnetization, with the peak sharpening as H_A falls relative to H_c. The inset in Fig. 2 plots ZFC magnetization at 7 kOe and 50 Oe, normalized to be unity at the maximum; this shows that the peak width is not changing quickly. The coercivity at 295 K is $\approx$800 Oe, yet measurements made an order of magnitude above and below this show the same cusp width.

The ZFC and FC magnetizations separate at T_{irr}, which is larger than the temperature of the maximum in either cusp. This is likely due to some small fraction of the sample having entered a ferromagnetic state at a temperature higher than that of the maximum of the cusp, since there will be a range of compositions and hence T_c's in the sample. It has been noted that in $La_{1-x}Sr_xCoO_3$ systems high-resolution electron microscopy indicates an inhomogeneous distribution of Sr^{2+} ions.[9,12] This would be expected to lead to a similarly inhomogeneous distribution of Co^{4+} which would lead to independent ferromagnetic regions in the sample which may differ in their T_c. In agreement with this, no impurity phases are evident from synchrotron XRD studies,[16] although the system may vary in composition about the mean. Thus, it is unlikely to be a two-phase system, with one phase antiferromagnetic and the other ferromagnetic. Other structural studies of isostructural $Ln_{1-x}Sr_xCoO_{3-\delta}$ phases reveal a range of solid solution ($x \geqslant 0.67$).[30] Hence there must be some randomness in the Sr^{2+} distribution (and therefore the Co^{3+} and Co^{4+} distributions), as the superstructure phase exists over a wide range of compositions. This gives an explanation for the divergence of ZFC from FC magnetization, as on cooling in zero field the ferromagnetic clusters will have no preferred orientation, giving a small ZFC magnetization, while cooling in a field causes the clusters to align, producing a larger magnetization as seen in Fig. 2.

Hence the system appears to contain ferromagnetic clusters in a nonferromagnetic matrix, with the clusters showing a range of magnetic ordering temperatures centered at $\approx$295 K. However, there is no need at this point to invoke glassiness. This is reinforced by Fig. 3 which shows the real (χ') and imaginary (χ'') parts of the ac susceptibility of $Y_{0.33}Sr_{0.67}CoO_{2.79}$ with $H_{AC}=6.25$ Oe, $H_{DC}=0$, and $f=125$ Hz. χ' shows a cusp at 295 K, and possibly a broad

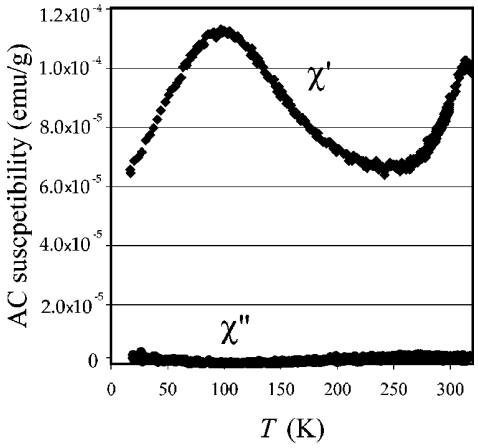

FIG. 4. ac susceptibility of $Y_{0.1}Sr_{0.9}CoO_{3-\delta}$, demonstrating the same features as Fig. 3 but the larger feature at 100 K, possibly larger due to the larger fraction of Co^{4+} ($\sim$45%).

feature centered at about 100 K, but χ'' shows no features whatsoever, indicating a lack of time dependence in the system and making glassiness unlikely. These measurements were repeated at a range of frequencies ($5 \leqslant f \leqslant 1000$ Hz) and all showed no feature in χ''.

So, with a Y:Sr ratio of 1:2 giving a small population of Co^{4+}, exchange interactions Co^{4+}-Co^{3+} would seem to be a small enough fraction that frustration and glassiness do not set in.

Spin state transitions have been observed in Co^{3+} perovskites, with those in $LaCoO_3$ gaining much attention (two recent examples are Refs. 31 and 32). There is the possibility of a broad feature in χ' in Fig. 3 centered at $\approx$100 K. It has been suggested that the dominant Co species in $LaCoO_3$ and its Sr-doped derivatives are intermediate spin (IS) Co^{3+} ($t_{2g}^5 e_g^1, S=1$) rather than high spin (HS, $t_{2g}^4 e_g^2, S=2$),[12,27,31] which allows a transition to HS. Similarly, it has been suggested that the Co^{4+} is in a low spin (LS) state ($S=1/2, t^5e^0$), which would also allow a transition to a higher spin state with T.

The effect is small and so only a relative handful of the ions can be participating. Sr^{2+} is a comparatively larger ion, so Sr-rich regions may favor larger, higher spin Co ions, with the energetics of the system balanced such that the small fraction of Co ions located in such regions undergo a spin state transition between 10 and 55 K.

It has been shown that for $Ln_{1-x}Sr_xCoO_{3-\delta}$ the fraction of Co^{4+} increases with increasing x.[30] Thus a preliminary experiment was performed on $Y_{0.1}Sr_{0.9}CoO_{3-\delta}$ ($\delta=0.23$, % $Co^{4+}=45$), in which its ac susceptibility was measured. This showed the same features as the $x=0.67$ sample: a sharp cusp at 310 K indicative of the onset of ferromagnetism and a broad feature centered at $\sim$100 K. The maximum at $\sim$100 K is larger relative to the transition at 310 K—compare Fig. 4 with Fig. 3—and the ferromagnetic response is larger for $x=0.9$ for all $T<T_c$, which would be expected with more Co^{4+}-Co^{3+} ferromagnetic double-exchange interactions present. The larger feature at 100 K does not correlate with a feature in χ'' and so could well be a spin state transition, while its increase in size relative to the cusp at 310 K also correlates with the extra Co^{4+}. This might appear to suggest that the spin state transition is in the Co^{4+}. However, if there is more ferromagnetically aligned Co^{3+} due to the greater fraction of ferromagnetic exchange interactions, then this would also lead to the spin transition having a larger signature at $x=0.67$. Hence which Co ions are undergoing the transition is not clear from these results.

C. Neutron diffraction

Neutron-diffraction patterns were collected at a range of temperatures from 10 to 480 K. Structural parameters varied smoothly with T, although interestingly the tetragonal ratio increased with T, such that $c/2a=1.0016(3)$ at 10 K and 1.0067(3) at 480 K. The structure was taken from Ref. 16 and their conclusions regarding lanthanide and oxygen vacancy distributions were found to be consistent with the ND data, although some details of atomic coordinates were slightly different. In summary, the $4e$ (0,0,z; $z\sim0.150$) site appears to be solely Y with the $4e$ (0,0,z; $z\sim0.628$) site being Sr and the $8g$ (0, 1/2, z; $z\sim0.132$) being mixed. ND also agreed that the oxygen vacancies were on the $8i$ (x,0,0; $x\sim0.260$) sites, although a large atomic displacement parameter for this site ($B_{iso}\sim5$ Å^2) suggested considerable disorder and possibly a larger fraction of vacancies than that determined by TGA; the TGA figure is used for consistency and because it is considered to be equally reliable. Bond valence calculations showed that the $8h$ Co sites (x,x,0; $x\sim0.242$, denoted Co1 sites in Ref. 16) are overbonded for Co^{3+}, indicating that this is the likely location of any Co^{4+}. This is supported by a direct examination of cobalt-oxygen bond lengths. At 350 K, the average Co1-O bond length (1.90 Å) is shorter than the average Co2-O bond length (1.97 Å). Oxidation of cobalt from Co^{3+} to Co^{4+} is accompanied by a reduction in ionic radii from 0.61 Å to 0.53 Å.[18] From TGA measurements 25% of the cobalt is present as Co^{4+}, and the observed smaller average Co1-O bond length indicates that the Co1 sites may be 50% Co^{4+}. In other words, Co^{4+} is limited to the Co1 sites only.

The refinement for 350 K is shown in Fig. 5(a).

The diffraction pattern at 10 K [Fig. 5(b)] shows a strong magnetic (112) reflection which is completely absent from the 350 K pattern. Other magnetic peaks revealed by subtraction included (116) and (224). Given that the structural cell is essentially a stack of $2\times2\times4$ perovskite cubes, each containing a single Co atom, this suggests a magnetic structure which is antiferromagnetic along each lattice direction—(112) being (111) in a $2\times2\times2$ unit cell, a conclusion born out by Rietveld analysis. The magnetic peak widths are consistent with that of the structural peaks, indicating that the antiferromagnetic magnetic order is long ranged.

Figure 6 plots $\sqrt{I_{112}}$ normalized to the value at 10 K against T/T_c, where $T_c=320$ K—larger than the 295 K from the ac susceptibility, but in keeping with the onset of Curie-Weiss behavior in the ZFC/FC data. The ac measurement is indicating the center of the distribution of T_c, which is at a lower temperature than the initial onset of ferromag-

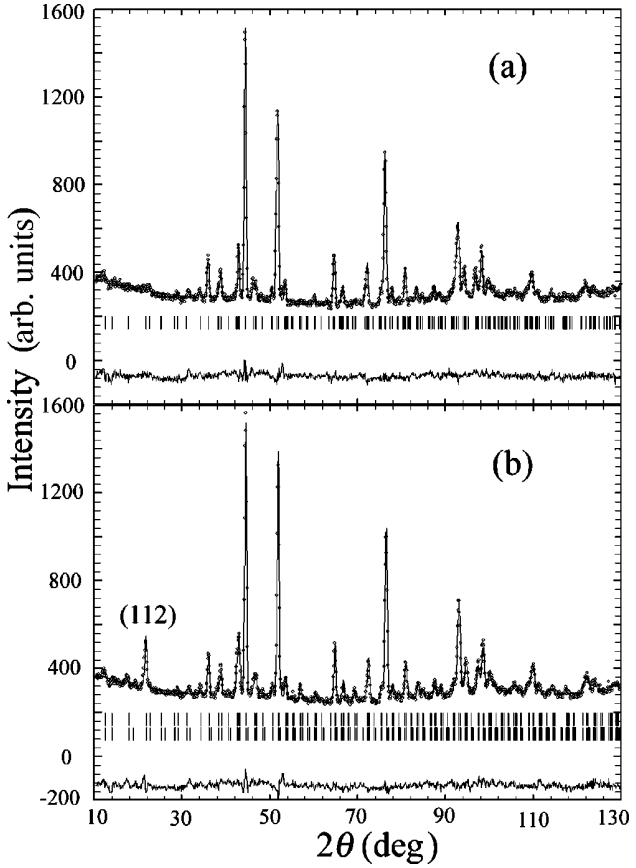

FIG. 5. Neutron-powder diffraction pattern (crosses) and fit and difference plot (solid lines) for $Y_{0.33}Sr_{0.67}CoO_{2.79}$ at (a) 350 K ($>T_c$) ($R_{\mathrm{Bragg}}=2.4$) and (b) 10 K ($R_{\mathrm{Bragg}}=2.7$, $R_M=5.4$). Markers give Bragg positions. Refinement uses the $I4/mmm$ cell outlined in Ref. 16. The second row of markers in (b) gives the Bragg peaks in $P\bar{1}$, as the magnetic symmetry was implemented by using this space group and specifying the moment symmetry explicitly using constraints.

netism. Superimposed are the Brillouin curves for $S=1$ (IS Co^{3+}) and $S=2$ (HS Co^{3+}). The difference is not large.

The refinements give a staggered moment per Co ion of $(2.0\pm0.3)\mu_B$. This is an average over *all* Co ions. It has been noted that a spin-only moment for $La_{1-x}Sr_xCoO_3$ would be $(2-x)\mu_B$ per Co assuming stoichiometry is maintained and the Co^{4+} is in a LS state and Co^{3+} in IS.[12] This would indicate that the antiferromagnetically correlated Co moments in $Y_{0.33}Sr_{0.67}CoO_{2.79}$ are in the main IS Co^{3+}.

Figure 6 and its inset show that I_{112} is marginally higher at 50 to 60 K ($0.15<T/T_c<0.2$) than at the lowest temperature, if the spread in values in the cluster of points at $T=50$ to 60 K is a measure of the error. Other peaks including the (224) peak show the same trend, although the errors are large due to small intensities. This is a further evidence for a spin state transition in the cobalt ions. Given that the effect is visible in the staggered magnetization, it is suggested that the transition is most likely a transition in the Co^{3+} from IS to HS, although it would appear that only a few percent of the ions in the long-range ordered antiferromagnetic lattice make the transition.

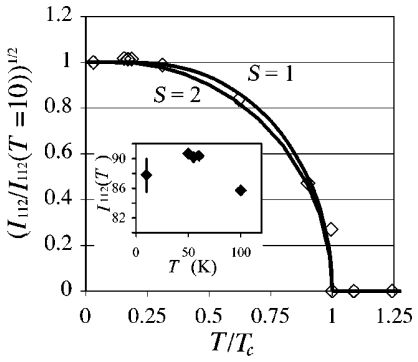

FIG. 6. (Magnetic intensity)$^{(1/2)}$ vs reduced temperature plotted for the (112) magnetic Bragg peak. Brillouin curves for $S=1$ and $S=2$ are included. Marker size in main figures gives error bars; an indicative error bar is shown in the inset.

The neutron magnetic powder diffraction data were analyzed using the Rietveld approach. Figure 5(b) shows a combined structural and magnetic refinement of $Y_{0.33}Sr_{0.67}CoO_{2.79}$ at 10 K. The upper row of peak markers gives the $I4/mmm$ peaks from the structural cell. The magnetic structure was implemented by using space group $P\bar{1}$ and explicitly constraining the magnetic moments to obey the appropriate symmetry, hence the high density of markers in the second row.

The system was found to be antiferromagnetic along all three lattice directions. The moments were found to be collinear and (anti)parallel with the c axis. This is effectively the G-type structure defined many years ago in the manganites.[33] The calculated neutron-diffraction profile in Fig. 5(b) is based on this model. Magnetometry results suggested that the ferromagnetism was not long-range ordered but clustered and so no ferromagnetism was initially explicitly incorporated into this model. It was added later as a test and found to add nothing to the quality of the fit, agreeing with the idea that the ferromagnetism exists in small regions.

It is therefore suggested that on cooling through ~320 K the system enters a long-range ordered antiferromagnetic state with Sr- and Co^{4+}-rich ferromagnetic regions which have a range of T_c's, giving a broad peak in the ZFC magnetization (Fig. 2), and T_{irr} greater than the temperature of the cusp. As the sample is cooled further, more of the Sr-rich regions become ferromagnetic but these data do not indicate that the sample goes to a state with a long-range ordered ferromagnetic component, although this may be masked in the diffraction pattern by the overlap of the (if present) small ferromagnetic Bragg peaks with the crystal-structural peaks. Short-ranged ferromagnetic order would be expected to lead to broad, diffuse regions of intensity at the base of each structural Bragg peak. However, such scattering would be difficult to observe unless very strong, and no unequivocal evidence can be found in these data.

IV. CONCLUSIONS

The magnetic properties of $Y_{0.33}Sr_{0.67}CoO_{2.79}$ have been outlined. In the magnetic state, the material shows M-H hys-

teresis, indicating ferromagnetism, and thermomagnetic hysteresis which can be explained by the presence of independent ferromagnetic regions in an antiferromagnetic matrix. Local variations in composition appear to give rise to a distribution of ferromagnetic transition temperatures. The lack of a cusp in the imaginary part of the ac susceptibility and the lack of a frequency dependence in the temperature of the cusp in the real part suggest that glassiness is absent. Hence, glassiness does *not* appear to be present, unlike many other rare-earth cobaltates.

The system orders predominantly antiferromagnetically below ≈ 320 K with an average staggered Co moment of $2\mu_B$. The antiferromagnetic order is long ranged, with the moments arranged collinearly in *G*-type antiferromagnetic structure,[33] (anti)parallel with the *c* axis.

A spin state transition may be present in the Co lattice, and is either due to the Co^{4+} or a small fraction of the Co^{3+} ions, with the latter considered more likely due to the transition being manifested in the antiferromagnetic Bragg peaks as well as the ac susceptibility.

ACKNOWLEDGMENTS

We would like to thank J. M. Cochrane (UNSW) and D. Cassidy (ANSTO) for technical support and R. L. Withers (ANU) for helpful discussions. D.J.G. thanks A. P. Heerdegen for useful advice. We acknowledge the financial support of AINSE Grant No. 02/140 and X.L.W. and D.J.G. acknowledge the support of the ARC.

*Also at The Bragg Institute, Australian Nuclear Science and Technology Organization, Lucas Heights, NSW 2234, Australia. Electronic address: goossens@rsc.anu.edu.au

[1] S.J. Skinner, Int. J. Inorg. Mater. **3**, 113 (2001).
[2] Y. Takeda, H. Ueno, N. Imanishi, O. Yamamoto, N. Sammes, and M.B. Philipps, Solid State Ionics **86-88**, 1187 (1996).
[3] R.H.E. van Doorn and A.J. Burggraaf, Solid State Ionics **128**, 65 (2000).
[4] S.B. Adler, Solid State Ionics **111**, 111 (1998).
[5] A.V. Kovalevsky, V.V. Kharton, V.N. Tikhonovich, E.N. Naumovich, A.A. Tonoyan, O.P. Reut, and L.S. Boginsky, Mater. Sci. Eng., B **52**, 105 (1998).
[6] V.V. Kharton, A.A. Yaremchenko, A.V. Kovalevsky, A.P. Viskup, E.N. Naumovich, and P.F. Kerko, J. Membr. Sci. **163**, 307 (1999).
[7] S. Mukherjee, R. Ranganathan, P.S. Anilkumar, and P.A. Joy, Phys. Rev. B **54**, 9267 (1996).
[8] K. Asai, O. Yokokura, N. Nishimori, H. Chou, G.S.J.M. Tranquada, S. Higuchi, Y. Okajima, and K. Kohn, Phys. Rev. B **50**, 3025 (1994).
[9] P.L. Kuhns, M.J.R. Hoch, W.G. Moulton, A.P. Reyes, J. Wu, and C. Leighton, Phys. Rev. Lett. **91**, 127202 (2003).
[10] G.H. Jonker and J.H. van Santent, Physica (Amsterdam) **19**, 120 (1953).
[11] M.A. Señarís-Rodríguez and J.B. Goodenough, J. Solid State Chem. **118**, 323 (1995).
[12] R. Caciuffo, D. Rinaldi, G. Barucca, J. Mira, J. Rivas, M.A. Señarís-Rodríguez, P.G. Radaelli, D. Fiorani, and J.B. Goodenough, Phys. Rev. B **59**, 1068 (1999).
[13] M. Itoh, I. Natori, S. Kubota, and M. Motoya, J. Phys. Soc. Jpn. **63**, 1486 (1994).
[14] P.S. Anil-Kumar, P.A. Joy, and S.K. Date, J. Phys.: Condens. Matter **10**, L487 (1998).
[15] S. Jeong, M.G. Kim, K.H. Kim, and C.H. Yo, Bull. Korean Chem. Soc. **17**, 794 (1996).
[16] R.L. Withers, M. James, and D.J. Goossens, J. Solid State Chem. **174**, 198 (2003).
[17] K.F. Wilson, D.J. Goossens, J.M. Cochrane, and M. James, in Proceedings of the 27th Annual AIP Condensed Matter and Materials Meeting 2003 (unpublished).
[18] R.D. Shannon, Acta Crystallogr., Sect. A: Found. Crystallogr. **32**, 751 (1976).
[19] See http://www.ncnr.nist.gov/resources/n-lengths/list.html
[20] M. Karpinnen, M. Matvejeff, K. Salomaeki, and H. Yamauchi, J. Mater. Chem. **12**, 1761 (2002).
[21] H.M. Rietveld, J. Appl. Crystallogr. **2**, 65 (1969).
[22] B.A. Hunter, IUCr Commission on Powder Diffraction Newsletter **20**, 21 (1998).
[23] J. Rodriguez-Carvajal, Physica B **192**, 55 (1993).
[24] S.Y. Istomin, J. Grins, G. Svensson, O.A. Drozhzhin, V.L. Kozhevnikov, E.V. Antipov, and J.P. Attfield, Chem. Mater. **15**, 4012 (2003).
[25] J.A. Mydosh, *Spin Glasses: An Experimental Introduction* (Taylor and Francis, London, 1993).
[26] A. Das, S.K. Paranjpe, P.A. Joy, and S.K. Date, J. Alloys Compd. **326**, 101 (2001).
[27] J. Wu and C. Leighton, Phys. Rev. B **67**, 174408 (2003).
[28] D.N.H. Nam, K. Jonason, P. Nordblad, N.V. Khiem, and N.X. Phuc, Phys. Rev. B **59**, 4189 (1999).
[29] S. Chaudhary, S.B. Roy, and P. Chaddah, J. Alloys Compd. **326**, 112 (2001).
[30] M. James, D. Cassidy, D.J. Goossens, and R.L. Withers (unpublished).
[31] C. Zobel, M. Kriener, D. Bruns, J. Baier, M. Grüninger, and T. Lorenz, Phys. Rev. B **66**, 020402(R) (2002).
[32] M. Itoh and J. Hashimoto, Physica C **341-348**, 2141 (2000).
[33] E.O. Wollan and W.C. Koehler, Phys. Rev. **100**, 545 (1955).